

Improved Aerodynamic Characteristics of Aerofoil Shaped Fuselage than that of the Conventional Cylindrical Shaped Fuselage

G.M. Jahangir Alam⁽¹⁾, Dr. Md. Mamun⁽²⁾ and Dr. A. K. M. Sadrul Islam⁽³⁾

Abstract— This paper is written to explain the aerodynamic characteristics of an Unmanned Air Vehicles (UAV) having “Aerofoil Shaped Fuselage” received numerically. This paper also compares that numerical result with that of the “Conventional Cylindrical Shaped Fuselage”. The proposed Aerofoil Shaped Fuselage is found to provide netter aerodynamic characteristics than that of the conventional cylindrical shaped fuselage. The aerofoil shaped fuselage could be used for designing the future UAV to use many military and civil applications. NACA 4416 cambered aerofoil with chord length of 100 mm has been used for this research purpose for all type of configuration design. The aerodynamic characteristics of Aerofoil Shaped Fuselage as well as Cylindrical Shaped Fuselage have been carried out at two different velocities (20 m/sec & 40 m/sec respectively) with different angle of attacks from -3° to 18° with 3° degree steps. The designs of both the models as well as numerical values have been obtained with the help of CFD software. The stalling angle for both the design is found at about 15° degree angle of attack for all the configurations. Finally some conclusions have been drawn on the basis of the computational result for both the designs.

Keywords— Unmanned Air Vehicles (UAV), Aerodynamic Design, Aerofoil Shaped Fuselage, Cylindrical Shaped Fuselage, Aerodynamic Characteristics, Lift Coefficient, Drag Coefficient, Angle of Attack, Stalling Angle.

1 INTRODUCTION

An air vehicle having no onboard pilot and capable of pre-programmed operation as well as reception of intermittent commands either independently or from a human operator at a distance from the ground is called Unmanned Air Vehicle (UAV). UAVs have been used to perform “dull, dirty and dangerous” missions successfully [1]. Recent advancement in communications, solid-state devices and battery technology have made small, low cost fixed wing UAVs which can provide important information for low-altitude and high resolution applications such as scientific data gathering, surveillance for law enforcement and homeland security, precision agriculture, forest fire monitoring, geological survey and many more scientific and commercial applications [2].

UAVs mostly fly under low speed conditions. The aerodynamic characteristics of the UAVs have many similarities than that of the monoplane configuration. Due to the UAV's potential for carrying out many tasks together without direct risk to the crew or humans in general, they are ideal for testing new concepts like “*Designing of Aerofoil Shaped Fuselage for UAV*” to analyze the further increase of the vehicle's capability [3] & [4].

UAV requires higher lifting force with a smaller size. As such, the concept of development of all lifting vehicle technology would bring good result for research on designing future UAV. The fuselage of UAV might be a good source of lifting

force. Hence, this paper will investigate and analyze the aerodynamic characteristics of an UAV having aerofoil shaped fuselage and compare the result with that of an UAV having conventional cylindrical shaped fuselage. The investigation has been carried out at two different velocities (20 m/sec & 40 m/sec respectively) and different angle of attacks from -3° to 18° with 3° degree steps.

2 COMPUTATIONAL DESIGN

NACA 4416 cambered aerofoil has been used for design and investigation of the aerodynamic characteristics of both aerofoil shaped fuselage & conventional cylindrical shaped fuselage configurations. The numerical data have been obtained by using Computational Fluid Dynamics (CFD) software. The flow of air through the aerofoils is considered to be incompressible and subsonic. The chord length of the aerofoil has been kept 10 cm. The total volume of both the models has been kept same, which is 534.102 cm^3 . The free stream air-flow has been kept 20 m/sec & 40 m/sec respectively and the effect of temperature has been neglected. The density of air has been considered $\rho_0 = 1.225 \text{ kg/m}^3$, operating pressure 1.01 bar or 14.7 psi and absolute viscosity $\mu = 1.789 \times 10^{-5} \text{ kg/m-s}$. The Reynold's Number has been considered 1.37×10^5 (for 20 m/sec) and 2.74×10^5 (for 40 m/sec) respectively. The data have been obtained at different angles of attack from -3° to 18° with 3° steps.

The design of both the models involves lot of trial & errors at different stages of the design. Modification of both the design have been carried out in different steps during creation of geometry & adjustment of far field boundary, meshing of geometry, setting up operation & boundary condition, setting up of different factors etc. Then, the variables of both the design have been initialized and checked for convergence. After ana-

1 G.M. Jahangir Alam, Department of Mechanical Engineering, MIST, Dhaka, Bangladesh, jahangiralam105@yahoo.com

2 Dr. Md. Mamun, Department of Mechanical Engineering, BUET, Dhaka, Bangladesh, mdmamun@me.buet.ac.bd

3 Dr. A. K. M. Sadrul Islam, Department of Mechanical and Chemical Engineering, Islamic University of Technology (IUT), Gazipur, Bangladesh, sadrul@iut-dhaka.edu

lyzing the result, the designed geometry has been further refined or re-meshed to obtain the accuracy as far as possible. As such, lot of trial & errors has been involved before finalization of a design. The finalized cylindrical and aerofoil shaped fuselage models have been converged after 200 & 190 iterations respectively. The finalized model UAV after meshing, different views of model UAV after meshing and grid display of both the models are shown in fig. 2.1 to 2.6 respectively.

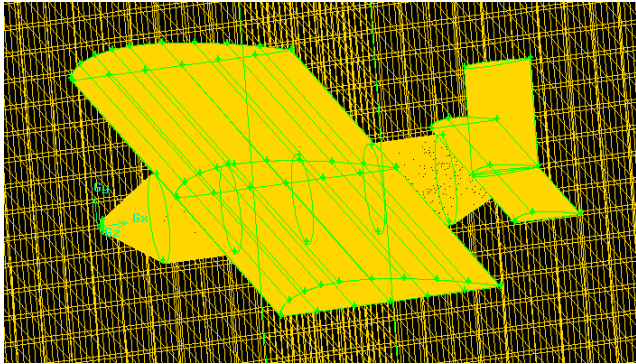


Fig. 2.1 Cylindrical Shaped Fuselage Model after Meshing.

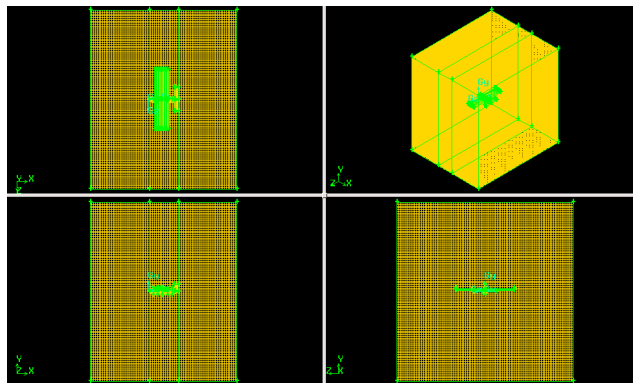


Fig. 2.2 Different Views of Cylindrical Shaped Fuselage Model after Meshing.

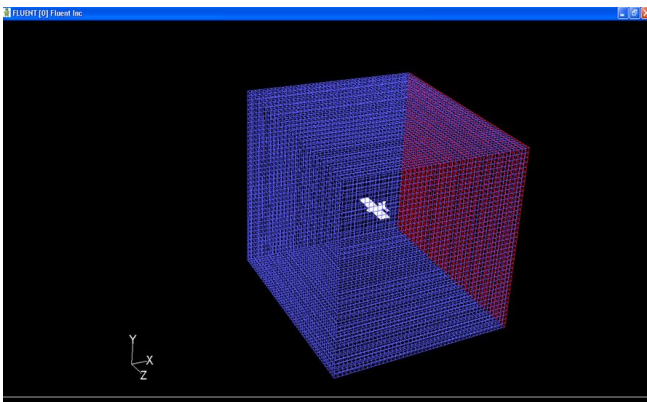


Fig. 2.3 Grid Display of Cylindrical Shaped Fuselage Model.

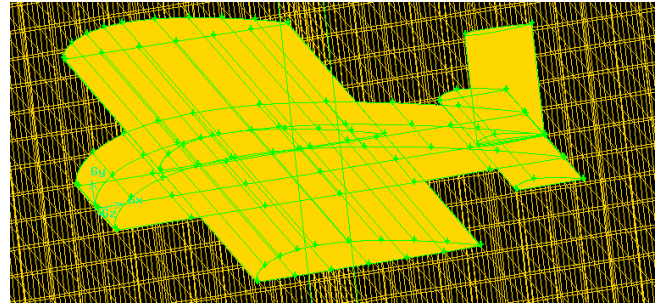


Fig. 2.4 Aerofoil Shaped Fuselage Model after Meshing.

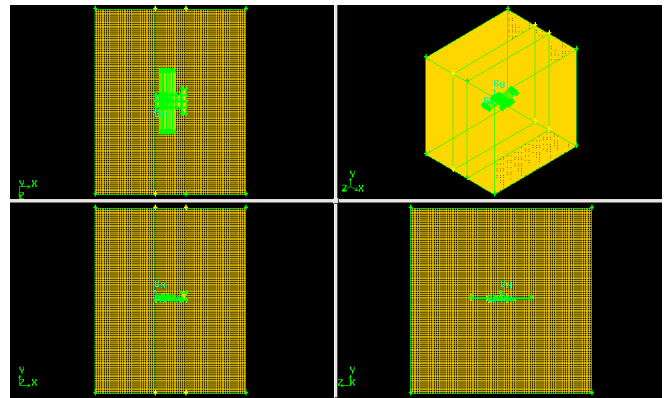


Fig. 2.5 Different Views of Aerofoil Shaped Fuselage Model after Meshing.

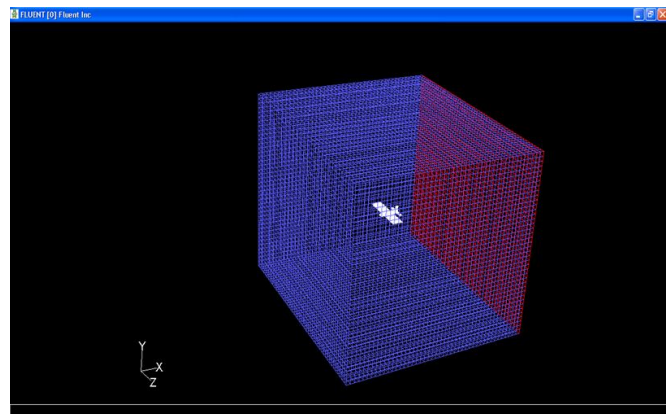


Fig. 2.6 Grid Display of Aerofoil Shaped Fuselage Model.

3 CONFIGURATION LAYOUT

3.1 Cylindrical Shaped Fuselage UAV Model

Four major parts of a typical cylindrical shaped fuselage UAV model are wing, fuselage, horizontal stabilizer and vertical stabilizer. Up wing type conventional model has been chosen. Total volume of this model is 534.102 cm^3 . The left and right wings have been designed by using NACA 4416 aerofoil. Major features which have been used during designing the wings of this model are as follows:

- Aerofoil type : NACA 4416 (cambered aerofoil).
- Chord Length : 10 cm.
- Tip to tip length of both wing : 44 cm.
- Center section diameter of fuselage : 4 cm.
- Root to tip length of each wing (span) : 20 cm.
- Maximum thickness between upper and lower surface: 1.186 cm.
- Taper Angle : Zero.

The shape of the designed conventional fuselage is cylindrical. It's nose to tail length is 20 cm. It has mainly three parts - divergent part, middle part and convergent part. Detail features use during designing the conventional fuselage is as follows:

- a. Divergent part (1st section)
 - Length : 2.8 cm.
 - Nose radius : Approx 0.25 cm.
 - Divergent angle : 25°.
- b. Middle part (2nd section)
 - Length : 13 cm.
 - Diameter : 4 cm (over the whole length).
- c. Convergent part (3rd section)
 - Length : 4.2 cm.
 - Tail radius : Approx zero.
 - Convergent angle : 22°.

Total length, width and thickness of horizontal stabilizer are 14 cm, 3 cm and 0.4 cm respectively. It has been placed in a suitable position at the rear side of the fuselage. Total length, width and thickness of vertical stabilizer are 6 cm, 3 cm and 0.8 cm respectively. It has also been placed in a suitable position at the rear side of the fuselage. The isometric of the cylindrical shaped fuselage UAV model is shown in fig. 3.1.

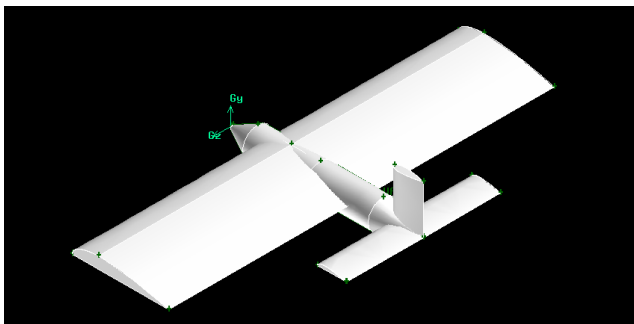


Fig. 3.1. Isometric View of Cylindrical Shaped Fuselage UAV Model.

3.2 Aerofoil Shaped Fuselage UAV Model

Four major parts of the proposed aerofoil shaped fuselage model are wing, fuselage, horizontal stabilizer and vertical stabilizer. Up wing type proposed model has been selected. The volume of the model is 534.102 cm³. The left and right wings have been designed by using NACA 4416 aerofoil. Major features use during designing the wings is as follows:

- Aerofoil type : NACA 4416 (cambered aerofoil).
- Chord Length : 10 cm.

- Thickness of fuselage : 8 cm.
- Tip to tip length of both wing : 48 cm.
- Root to tip length of each wing (span) : 20 cm.
- Maximum thickness between upper and lower surface : 1.186 cm.
- Taper Angle : Zero.

The fuselage of this model is also aerofoil shaped. It's chord length is 20 cm. The left and right fuselages have been designed by using NACA 4416 aerofoil. Major features use during designing the fuselage is as follows:

- Aerofoil type : NACA 4416 (cambered aerofoil).
- Chord Length : 20 cm.
- Tip to tip length of both fuselage : 8 cm.
- Root to tip length of each fuselage (span) : 4 cm.
- Maximum thickness between upper and lower surface : 2.26 cm.
- Taper Angle : Zero.

Total length, width and thickness of horizontal stabilizer are 14 cm, 3 cm and 0.4 cm respectively. It has been placed in a suitable position at the rear side of the fuselage. Total length, width and thickness of vertical stabilizer are 6 cm, 3 cm and 0.8 cm respectively. It has been also placed in a suitable position at the rear side of the fuselage. The isometric view of the aerofoil shaped fuselage UAV model is shown in fig. 3.2.

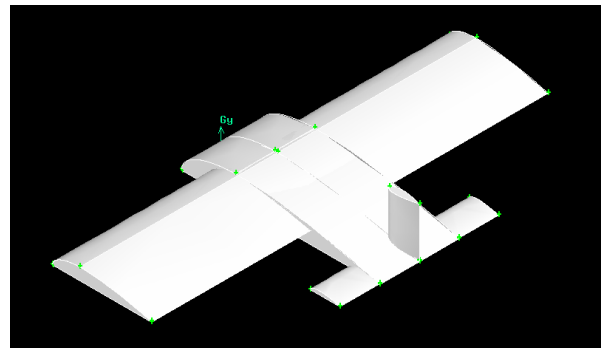


Fig. 3.2. Isometric View of Aerofoil Shaped Fuselage UAV Model

4 AERODYNAMIC CHARACTERISTICS

4.1 Aerodynamic Characteristics of Cylindrical Shaped Fuselage Model at 20 m/sec

The variation of lift coefficient with angle of attack at 20 m/sec for conventional cylindrical shaped fuselage model at different angle of attack is shown in fig. 4.1. The zero lift angle has been found at -3° angle of attack. Then the lift coefficient increases almost linearly with the increase of angle of attack up to approximately 15°. In other words, the lift coefficient increases linearly with the increase of angle of attack up to 15°. After wards, the lift coefficient decreases with the further increase of angle of attack. As such, the stalling angle of conventional cylindrical shaped fuselage model is found at about 15°. It is also observed that the maximum lift coefficient, C_{Lmax} for this type of model is approximately 0.946.

ly 1.109.

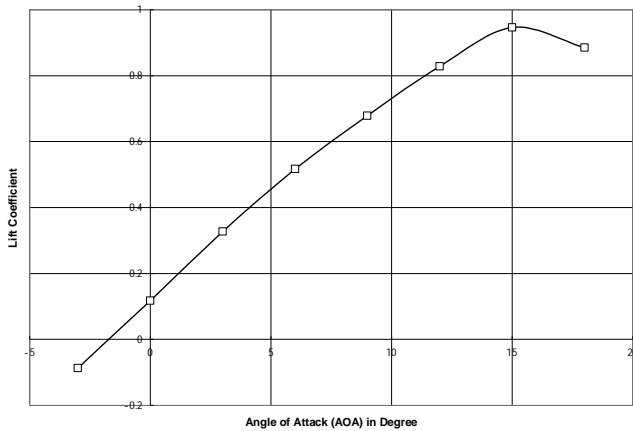


Fig. 4.1. Variation of Lift Coefficient with Angle of Attack for Cylindrical Shaped Fuselage Model at 20 m/sec.

The variation of drag coefficient with angle of attack at 20 m/sec for conventional cylindrical shaped fuselage model at different angle of attack is shown in fig. 4.2. The shape of the drag coefficient vs angle of attack curve is found parabolic nature. As such, the drag coefficient increases with the increase of angle of attack. The value of drag coefficient for this model at 15° angle of attack is found 0.144.

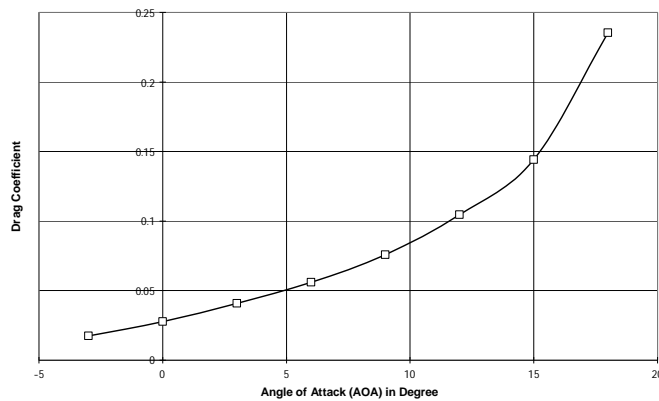


Fig. 4.2. Variation of Drag Coefficient with Angle of Attack for Cylindrical Shaped Fuselage Model at 20 m/sec.

4.2 Aerodynamic Characteristics of Cylindrical Shaped Fuselage Model at 40 m/sec

The variation of lift coefficient with angle of attack at 40 m/sec for conventional cylindrical shaped fuselage model at different angle of attack is shown in fig. 4.3. The zero lift angle has been found at -3° angle of attack. Then the lift coefficient increases almost linearly with the increase of angle of attack up to approximately 15°. In other wards, the lift coefficient increases linearly with the increase of angle of attack up to 15°. After wards, the lift coefficient decreases with the further increase of angle of attack. As such, the stalling angle of this model is found at about 15°. It is also observed that the maximum lift coefficient, C_{Lmax} for this type of model is approximate-

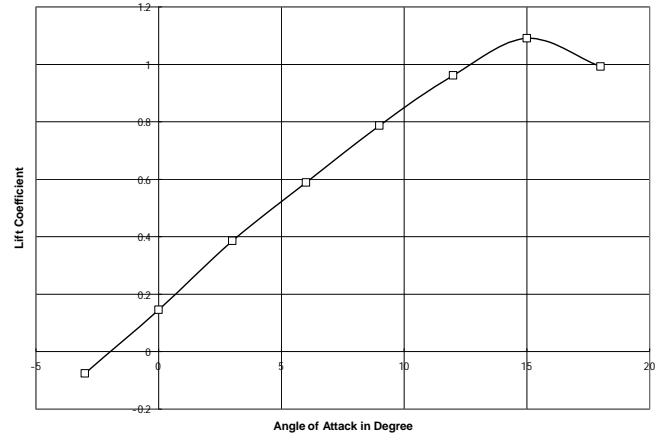


Fig. 4.3. Variation of Lift Coefficient with Angle of Attack for Cylindrical Shaped Fuselage Model at 40 m/sec.

The variation of drag coefficient with angle of attack at 40 m/sec for conventional cylindrical shaped fuselage model at different angle of attack is shown in fig. 4.4. The shape of the drag coefficient vs angle of attack curve is found parabolic nature. As such, the drag coefficient increases with the increase of angle of attack. The value of drag coefficient for this model at 15° angle of attack is found 0.134.

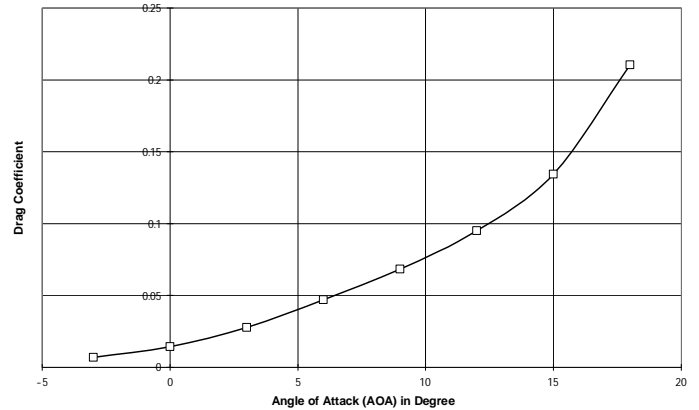


Fig. 4.4. Variation of Drag Coefficient with Angle of Attack for Cylindrical Shaped Fuselage Model at 40 m/sec.

4.3 Aerodynamic Characteristics of Aerofoil Shaped Fuselage Model at 20 m/sec

The variation of lift coefficient with angle of attack at 20 m/sec for aerofoil shaped fuselage model at different angle of attack is shown in fig. 4.5. The zero lift angle has been found at -3° angle of attack. Then the lift coefficient increases almost linearly with the increase of angle of attack up to approximately 15°. In other wards, the lift coefficient increases linearly with the increase of angle of attack up to 15°. After wards, the lift coefficient decreases with the further increase of angle of attack. As such, the stalling angle of aerofoil shaped fuselage model is found at about 15°. It is also observed that the maximum lift coefficient, C_{Lmax} for this type of model is approximate-

ly 1.20.

for this type of model is approximately 1.221.

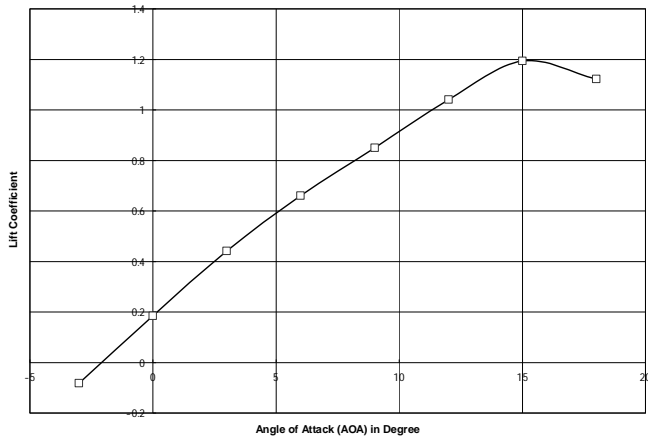


Fig. 4.5. Variation of Lift Coefficient with Angle of Attack for Aerofoil Shaped Fuselage Model at 20 m/sec.

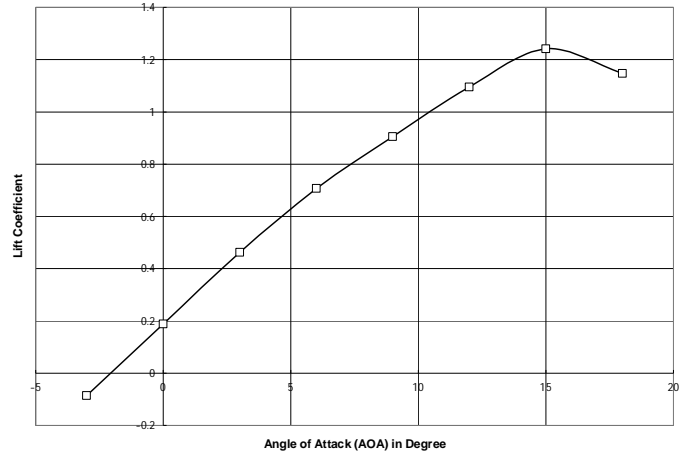


Fig. 4.7. Variation of Lift Coefficient with Angle of Attack for Aerofoil Shaped Fuselage Model at 40 m/sec.

The variation of drag coefficient with angle of attack at 20 m/sec for aerofoil shaped fuselage model at different angle of attack is shown in fig.4.6. The shape of the drag coefficient vs angle of attack curve is found parabolic. As such, the drag coefficient increases with the increase of angle of attack. The value of drag coefficient for this aerofoil shaped fuselage model at 15° angle of attack is found 0.234.

The variation of drag coefficient with angle of attack at 40 m/sec for aerofoil shaped fuselage model at different angle of attack is shown in fig. 4.8. The shape of the drag coefficient vs angle of attack curve is found parabolic nature. As such, the drag coefficient increases with the increase of angle of attack. The value of drag coefficient for this proposed model at 15° angle of attack is found 0.165.

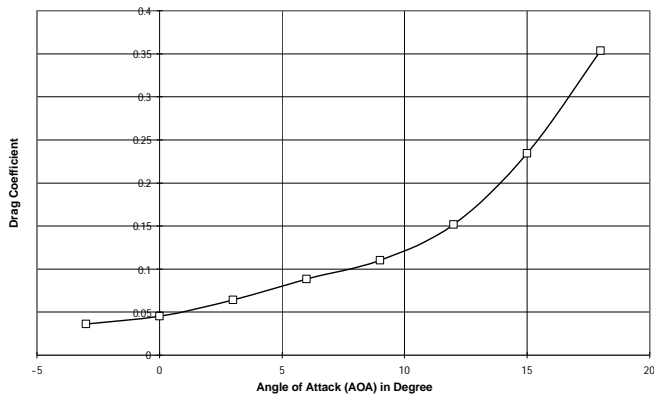


Fig. 4.6. Variation of Drag Coefficient with Angle of Attack for Aerofoil Shaped Fuselage Model at 20 m/sec.

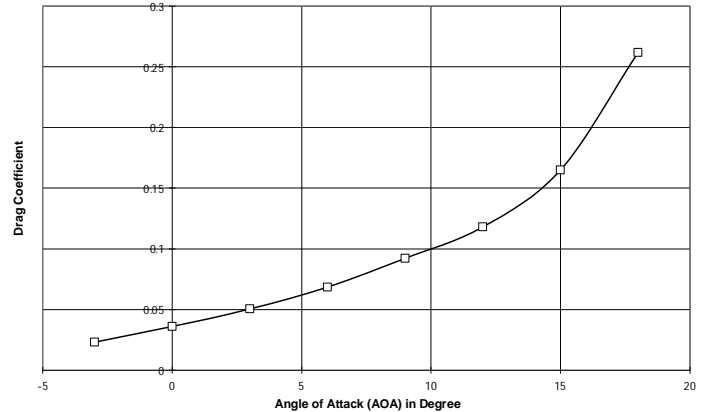


Fig. 4.8. Variation of Drag Coefficient with Angle of Attack for Aerofoil Shaped Fuselage Model at 40 m/sec.

4.4 Aerodynamic Characteristics of Aerofoil Shaped Fuselage Model at 40 m/sec

The variation of lift coefficient with angle of attack at 40 m/sec for aerofoil shaped fuselage model at different angle of attack is shown in fig. 4.7. The zero lift angle has been found at -3° angle of attack. Then the lift coefficient increases almost linearly with the increase of angle of attack up to approximately 15°. In other words, the lift coefficient increases linearly with the increase of angle of attack up to 15°. After wards, the lift coefficient decreases with the further increase of angle of attack. As such, the stalling angle of this model is found at about 15°. It is also observed that the maximum lift coefficient, C_{Lmax}

5 ANALYSIS OF RESULT

5.1 Comparison of Lift Coefficient of Different Models

The comparison of lift coefficient with angle of attack of different models at two different velocities is shown in fig.5.1. The zero lift angle has been found approximately at -3° angle of attack. Then the lift coefficient increases almost linearly with the increase of angle of attack up to 15°. Among the two configurations, the aerofoil shaped fuselage has produced more lift coefficient than that of the cylindrical shaped fuselage. The aerofoil shaped fuselage model produced a significant amount of extra lift from it's fuselage due to aerofoil shape. Among the

four studies, maximum lift coefficient is produced by the aerofoil shaped fuselage model at 40 m/sec. Next increment of lift coefficient is provided by the aerofoil shaped fuselage model at 20 m/sec and next to next is provided by the cylindrical shaped fuselage at 40 m/sec. The cylindrical shaped fuselage provides minimum lift coefficient at 20 m/sec among the four types of studies. As such, improved aerodynamic characteristics is observed from the aerofoil shaped fuselage and such model may be used for designing the future UAV.

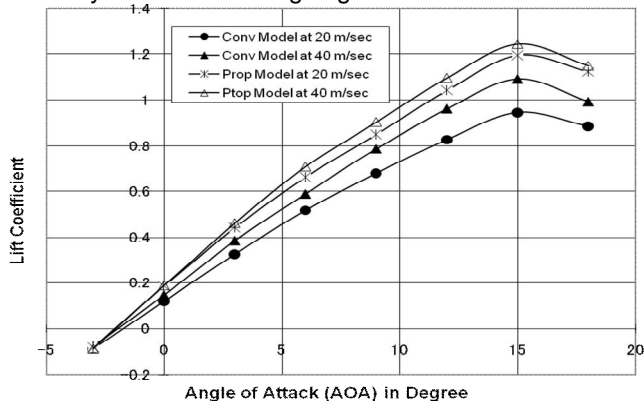


Fig. 5.1. Comparison of Lift Coefficient with AOA of Different Models.

5.2 Comparison of Drag Coefficient of Different Models

The comparison of drag coefficient with angle of attack of different models at two different velocities is shown in fig. 5.2. The shape of the drag coefficient vs angle of attack curve is found parabolic. As such, the drag coefficient increases with the increase of angle of attack. Among the two configurations, the aerofoil shaped fuselage has produced more drag coefficient than that of the cylindrical shaped fuselage. Drag coefficient of aerofoil shaped fuselage is found more due to increase of induced drag for trailing edge vortices from aerofoil shaped fuselage. However, profile drag of both the models is same as both the models has the same volume. Among the four studies, maximum drag coefficient is produced by the aerofoil shaped fuselage model at 20 m/sec. It is because flow separation starts earlier for aerofoil shaped fuselage model at 20 m/sec. Out of four studies, next drag coefficient is found more for the aerofoil shaped fuselage model at 40 m/sec and next to next is found for cylindrical shaped fuselage at 20 m/sec. Cylindrical shaped fuselage at 40 m/sec provides minimum drag coefficient among the four types of studies.

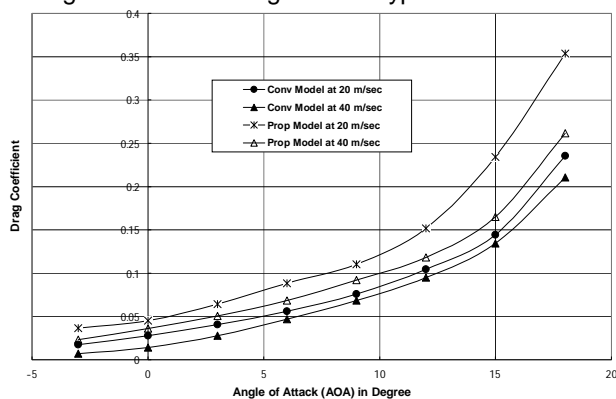


Fig. 5.2. Comparison of Drag Coefficient with AOA of Different Models.

5.3 Lift to Drag Ratio Curve of Different Models

The lift to drag ratio curves of aerofoil shaped fuselage and cylindrical shaped fuselage models are shown from fig. 5.3 to 5.6 respectively. The lift to drag coefficient is found less for aerofoil shaped fuselage model due to increase of induced drag for trailing edge vortices from the aerofoil shaped fuselage. However, profile drag of both the models is same as both the models has the same volume. But said model also increased a significant amount of extra lift from its fuselage due to aerofoil shape. From all the graphs, it is found that both the lift and drag coefficient increase almost linearly up to stall angle. Afterwards, a sharp increase of drag coefficient with reduction of lift coefficient occurs for all the configurations ie separation of flow starts after the stalling angle. Table-1 shows the lift to drag ratio of all the configurations at the stalling angle.

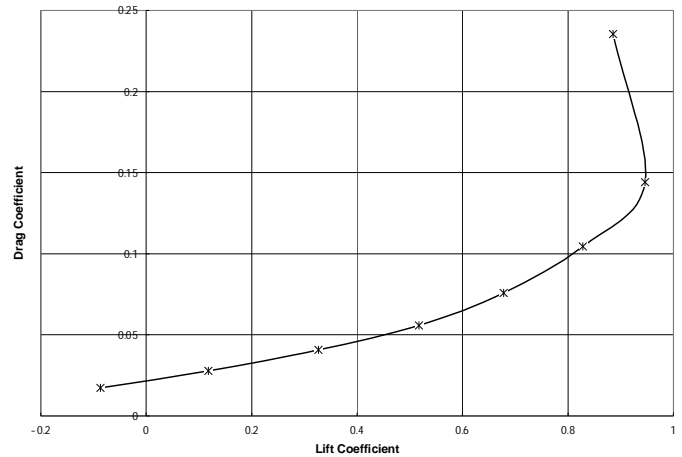


Fig. 5.3. Lift to Drag Ratio Curve of Cylindrical Shaped Fuselage Model at 20 m/sec

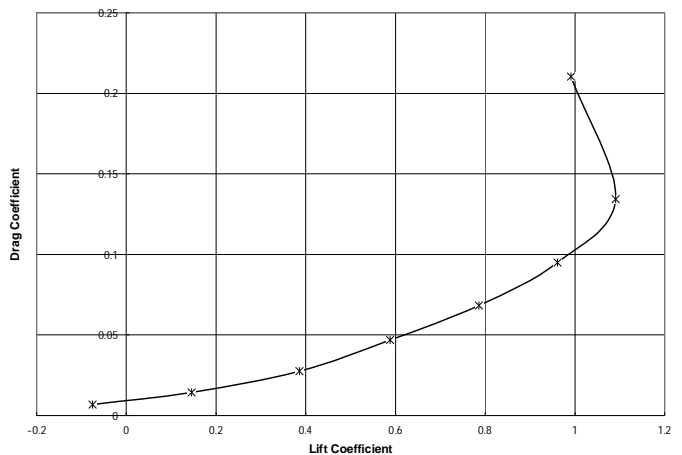


Fig. 5.4. Lift to Drag Ratio Curve of Cylindrical Shaped Fuselage Model at 40 m/sec

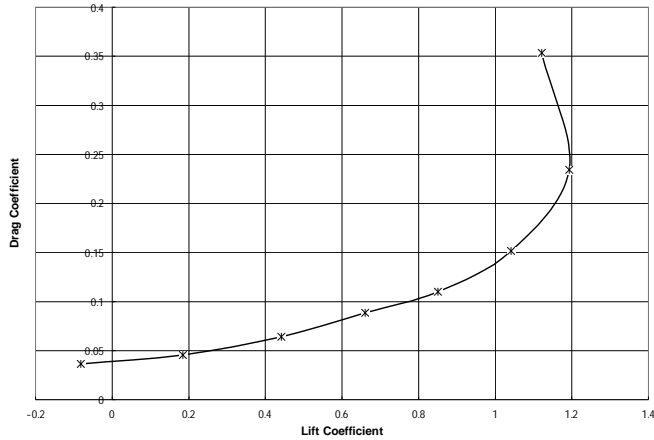


Fig. 5.5. Lift to Drag Ratio Curve of Aerofoil Shaped Fuselage Model at 20 m/sec

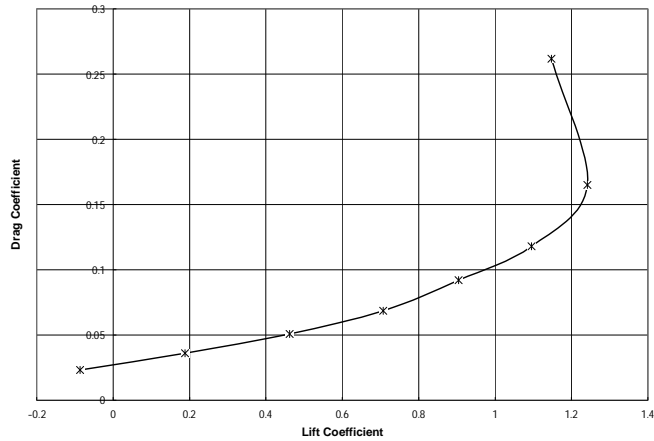


Fig. 5.6. Lift to Drag Ratio Curve of Aerofoil Shaped Fuselage Model at 40 m/sec

Configurations	Stall Angle	C_{Lmax}	C_{Dmax}	L/D Ratio
Conventional Model at 20 m/sec	15.0°	0.946	0.144	6.57
Conventional Model at 40 m/sec	15.0°	1.109	0.134	8.28
Proposed Model at 20 m/sec	15.0°	1.20	0.234	5.13
Proposed Model at 40 m/sec	15.0°	1.221	0.165	7.40

Table-1. Lift to Drag Ratio of all the Four Configurations at the Stalling Angle.

5.4 Increment of Lift and Drag Coefficient by Aerofoil Shaped Fuselage Model at 20 m/sec

Percentage increase of lift and drag coefficient of aerofoil shaped fuselage model at 20 m/sec than that of conventional cylindrical shaped fuselage model at different angle of attack

are shown in fig. 5.7 and 5.8 respectively. The aerofoil shaped fuselage configuration provides more lift as well as drag coefficient than that of the conventional cylindrical shaped fuselage configuration. From fig. 5.7, it is observed that out of two different studies, the percentage increment of lift coefficient is more for 'aerofoil shaped fuselage configuration at 20 m/sec' than that of the 'conventional cylindrical shaped fuselage' at velocity 20 m/sec & 40 m/sec respectively. Again from fig. 5.8, it is also observed that the percentage increment of drag coefficient is found more for 'aerofoil shaped fuselage configuration at 20 m/sec' than that of the 'conventional cylindrical shaped fuselage' at velocity 20 m/sec & 40 m/sec respectively. It is also seen from fig. 5.7 that 'aerofoil shaped fuselage configuration at 20 m/sec' provides approximately 20.73% & 8.62% more lift force coefficient at 15° angle of attack (stall angle) than that of the conventional cylindrical shaped fuselage configuration at velocity 20 m/sec & 40 m/sec respectively. It is also found from fig. 5.8 that the 'aerofoil shaped fuselage configuration at 20 m/sec' provides approximately 38.42% & 42.66% more drag coefficient at 15° angle of attack (stall angle) than that of the conventional cylindrical shaped fuselage configuration at velocity 20 m/sec & 40 m/sec respectively.

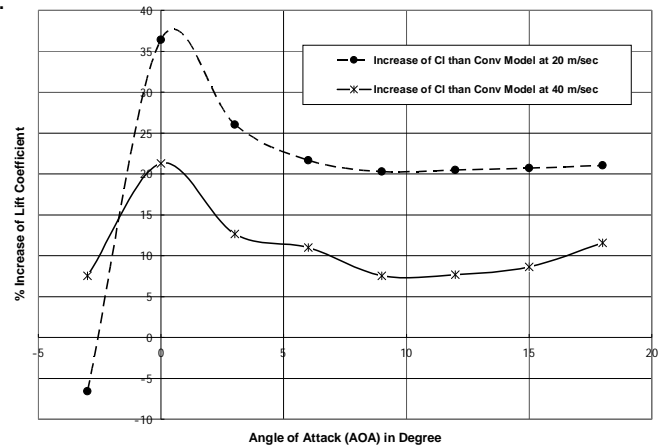


Fig. 5.7 Percentage Increase of Lift Coefficient of "Aerofoil shaped fuselage configuration at 20 m/sec" than that of "Cylindrical shaped fuselage configuration at 20 m/sec & 40 m/sec" respectively and Different Angle of Attack.

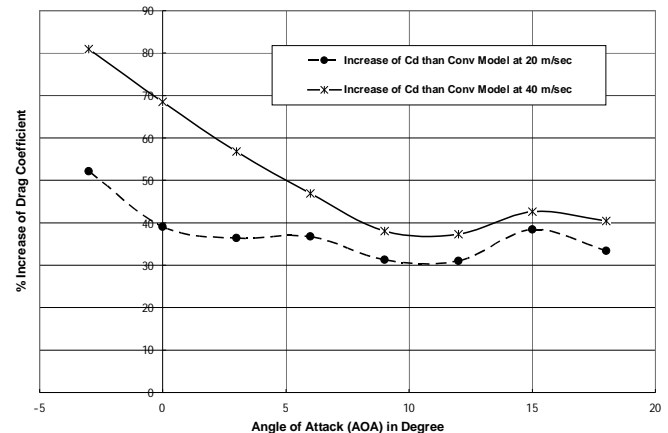


Fig. 5.8 Percentage Increase of Drag Coefficient of “Aerofoil shaped fuselage configuration at 20 m/sec” than that of “Cylindrical shaped fuselage configuration at 20 m/sec & 40 m/sec” respectively and Different Angle of Attack.

5.5 Increment of Lift and Drag Coefficient by Aerofoil Shaped Fuselage Model at 40 m/sec

From fig. 5.9, it is observed that out of two different studies, the percentage increment of lift coefficient is found more for ‘aerofoil shaped fuselage configuration at 40 m/sec’ than that of ‘conventional cylindrical shaped fuselage’ at velocity 20 m/sec & 40 m/sec respectively. Again from fig. 5.10, it is also observed that the percentage increment of drag coefficient is more for ‘aerofoil shaped fuselage configuration at 40 m/sec’ than that of ‘conventional cylindrical shaped fuselage’ at velocity 20 m/sec & 40 m/sec respectively. It is seen from fig. 5.9 that the ‘aerofoil shaped fuselage configuration at 40 m/sec’ provides approximately 23.79% & 12.15% more lift coefficient at 15° angle of attack (stall angle) than that of the conventional cylindrical shaped fuselage configuration at velocity 20 m/sec & 40 m/sec respectively. It is also found from fig. 5.10 that the ‘aerofoil shaped fuselage configuration at 40 m/sec’ provides approximately 12.62% & 18.64% more drag coefficient at 15° angle of attack (stall angle) than that of the conventional cylindrical shaped fuselage configuration at velocity 20 m/sec & 40 m/sec respectively.

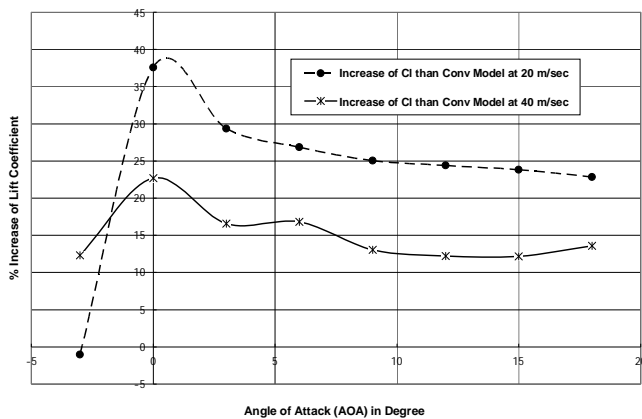


Fig. 5.9: Percentage Increase of Lift Coefficient of “Aerofoil shaped fuselage configuration at 40 m/sec” than that of “Cylindrical shaped fuselage configuration at 20 m/sec & 40 m/sec” respectively and Different Angle of Attack.

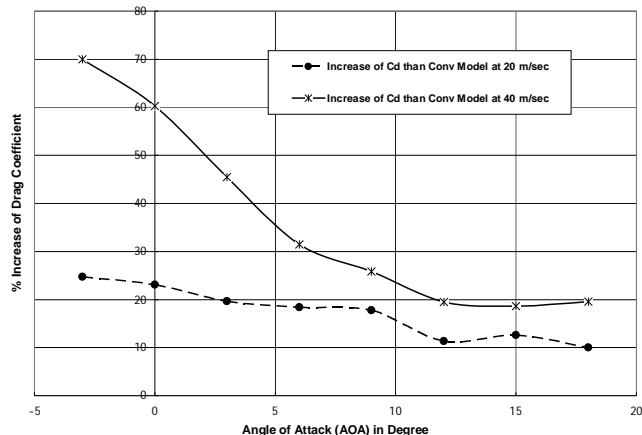


Fig. 5.10: Percentage Increase of Drag Coefficient of “Aerofoil shaped fuselage configuration at 40 m/sec” than that of “Cylindrical shaped fuselage configuration at 20 m/sec & 40 m/sec” respectively and Different Angle of Attack.

6 CONCLUSIONS

UAV requires higher lifting force with a smaller size. In order to maximize the efficiency of an UAV - the concept of development of all lifting vehicle technology might bring good result for designing of future UAV. For this reason, the aerofoil shaped fuselage of an UAV might be a good source of lifting force.

This paper explains the aerodynamic characteristics of a low speed aerofoil shaped fuselage and compare the result with that of the conventional cylindrical shaped fuselage. NACA 4416 aerofoil profile and CFD software have been used for both the design. The investigation has been carried out at 20 m/sec & 40 m/sec respectively and the volume of both the models has been kept same. The angle of attack has been varied from -3° to 18° with 3° steps. The stalling angle for both the designs is found at about 15°.

The ‘aerofoil shaped fuselage configuration at 20 m/sec’ provides approximately 20.73% & 8.62% more lift coefficient at 15° angle of attack (stall angle) than that of the conventional cylindrical shaped fuselage configuration at velocity 20 m/sec & 40 m/sec respectively. The ‘aerofoil shaped fuselage configuration at 20 m/sec’ also provides approximately 38.42% & 42.66% more drag coefficient at 15° angle of attack (stall angle) than that of the conventional cylindrical shaped fuselage configuration at velocity 20 m/sec & 40 m/sec respectively.

The ‘aerofoil shaped fuselage configuration at 40 m/sec’ provides approximately 23.79% & 12.15% more lift coefficient at 15° angle of attack (stall angle) than that of the conventional cylindrical shaped fuselage configuration at velocity 20 m/sec & 40 m/sec respectively. The ‘aerofoil shaped fuselage configuration at 40 m/sec’ also provides approximately 12.62% & 18.64% more drag coefficient at 15° angle of attack (stall angle) than that of the conventional cylindrical shaped fuselage configuration at velocity 20 m/sec & 40 m/sec respectively.

The aerofoil shaped fuselage has produced more lift coefficient than that of the conventional cylindrical shaped fuselage. It has produced a significant amount of extra lift from its fuselage due to aerofoil shape. But said model has also produced some extra drag due to increased fuselage frontal area, fuselage-wing interference effect and trailing edge vortex. The effect of fuselage frontal area is found minimum for UAV as it is smaller in size. The fuselage-wing interference effect has been reduced by selecting the up wing type model. However, ways for reduction of the trailing edge vortex from aerofoil shaped fuselage might be investigated in future to enhance the efficiency further more. As such, it could be easily told that the aerofoil shaped fuselage might be a very good option for designing the future UAV.

REFERENCES

- [1] Jodi A. Miller, Paul D. Minear, Albert F. Niessner, Jr, Anthony M. DeLullo, Brian R. Geiger, Lyle N. Long and Joseph F. Horn, "Intelligent Unmanned Air Vehicle Flight Systems", *Journal of Aerospace Computing, Information and Communication*, pp. 816-823, May 2007.
- [2] Beard Randal, Derek Kingston, Morgan Quigley, Deryl Snyder, Reed Christiansen, Walt Johnson, Timothy McLain and Michael A. Goodrich, "Autonomous Vehicle Technologies for Small Fixed-Wing UAVs", *Journal of Aerospace Computing, Information and Communication*, pp. 92-94, January 2005.
- [3] M. Secanell, A. Suleman and P. Gamboa "Design of a Morphing Airfoil for a Light Unmanned Aerial Vehicle using High-Fidelity Aerodynamic Shape Optimization" *Journal of American Institute of Aeronautics and Astronautics (AIAA 2005-1891)*, pp. 1-20, April 2005.
- [4] Agarwal Ramesh "Computational Fluid Dynamics of Whole-Body Aircraft" *Annu. Rev. Fluid Mech*, pp. 125-136, 1999.